Correlation Analysis of Chemical Bonds (CACB) II: Quantum Mechanical Operators for Classical Chemical Concepts

Terumasa Yamasaki

Asahi Chemical Ind. Co., Ltd., 2-1 Samejima, Fuji, Shizuoka 416-8501, Japan

Daniel T. Mainz and William A. Goddard, III*

Materials and Process Simulation Center, Beckman Institute (139-74), California Institute of Technology, Pasadena, California 91125

Received: December 1, 1999

We apply correlation analysis of chemical bonds (CACB) to simple organic reaction paths. CACB, an operator-based formalism for analyzing the electronic structure for molecule, clarifies how bond exchange processes relate to changes in covalent bond orders and bond interaction coefficients. For single bond-exchange processes, the *bonds correlation* typically is negative for interchanging bonds. For two bond-exchange processes, this coefficient can be either negative or slightly positive near zero, reflecting the nature of the bond exchange process. The simplest formalism can, sometimes, lead to unphysical values for the atomic valence and the bonds correlation coefficients. We analyzed the origin of this behavior and attributed it to the non-Hermitian property of the operator. We show how to avoid this problem by symmetrizing the operator through use of orthogonal atomic orbitals.

1. Introduction

The advances in quantum chemistry now provide chemical accuracy for the geometry, energies, and other properties of molecules. Indeed, it has become routine to obtain accurate energetics for reaction rates and solvation energies. In some cases, the predictions have been used to conceive new synthetic routes and design new catalysts. Despite these advances, interpretation of the wave function in terms of such simple concepts as atomic valence and bond crossing in reactions still lags far behind. Theoretical approaches to extracting the underlying chemical concept out of the immense amount of data output from such computations are scarce and unpersuasive. Since such chemical concepts are essential and indispensable to the reasoning about molecular properties and chemical reactivities, it is important to find ways of using rigorous quantum mechanical analyses to extract such chemical concepts.[1−10]

Quantum mechanical observables are associated with Hermitian operators. With a given wave function, the physical quantity is readily determined by computing the expectation value for the operator. On the other hand, empirical chemical concepts, such as the charge on an atom or the bond order on a molecule, are not necessarily associated with such operator representations. Rather, these concepts have been developed empirically over the history of chemistry to provide insight and relationship into complicated chemical phenomena.

Several attempts have been made to express the electronic structure of a molecule by an operator-based description,[1,3−5] including the correlation analysis of chemical bonds (CACB).[1] In the CACB formalism, the electronic character of a molecule (including its chemical reactivity) is expressed by a hierarchy of operators which begins with the atomic charge operator. This hierarchy includes the chemical bond operator and the *bonds correlation* operator, where each operator is defined in terms of the statistical covariance of the previous operator. Here the bonds correlation relates to bond exchange processes of chemical reactions. Thus, atomic, bond, and reactivity concepts are described by a consistent algebraic structure of operators.

Previously, we presented the CACB methodology with applications to simple organic and inorganic molecules. As CACB begins with the atomic charge operator, the whole description of electronic structure depends on the choice of the charge operator. This operator could be taken as the Mulliken charge operator or as the natural atomic orbitals (NAO) charge operator, or as some other operator that leads to intuitively useful charges. The criterion for which operator is best may be based on distribution of bonds and bonds correlations and how they change in various chemical processes.

In this paper we discuss the importance of using a Hermitian charge operator to obtain physically meaningful results for chemical reactions. Section 3 demonstrates the problem that can occur from using non-Hermitian charge operators. Section 4 applies the CACB hierarchical descriptive scheme for the analysis of several chemical reaction paths.

2. Overview of the Method

The details of the CACB methodology were presented previously.[1] Here we will summarize the formalism and definitions.

We start with a definition of the atomic charge, Q_A, as the expectation value of an atomic charge operator, $\hat{q}_A$, such that the values of Q_A correspond reasonably well to common concepts.

$$Q_A = \langle \hat{q}_A \rangle \tag{1}$$

The bra ($\langle$) and ket ($\rangle$) denote $\langle HF|$ and $|HF\rangle$, respectively. The formalism can be applied to general wave functions, but we consider only single determinants here. A particular form of the atomic charge operator is the *Mulliken charge operator*, which yields Mulliken gross atomic populations upon summa-

10.1021/jp9942320 CCC: $19.00
Published on Web 02/19/2000

tion over the atomic orbitals on A.

$$\hat{q}_A = \sum_a^A a^+ \bar{a}^- \quad \langle \hat{q}_A \rangle = Q_A \tag{2}$$

The creation and annihilation operators satisfy the commutation relations in

$$\begin{aligned} a^+\bar{b}^+ + \bar{b}^+ a^+ &= 0 \\ a^-\bar{b}^- + \bar{b}^- a^- &= 0 \\ a^+\bar{b}^- + \bar{b}^- a^+ &= \delta_{a,b} \end{aligned} \tag{3}$$

which employs a mixed covariant and contravariant basis ($\langle a|\bar{b}\rangle = \delta_{ab}$) since atomic orbitals are generally nonorthogonal [for orthogonal atomic orbitals, $a = \bar{a}$].[11]

A second choice for defining the atomic charge operator leads to NAO charges.[6] The *NAO charge operator* is preferred over the Mulliken charge operator for use with CACB formalism,[1] since NAO provides an orthogonal AO set with core (c_A) and valence (v_A) functions well localized on each atom.[6]

$$\hat{q}_A = \sum_c^{\text{core}} c_A^+ c_A^- + \sum_v^{\text{valence}} v_A^+ v_A^- + \sum_r^{\text{rydberg}} r_A^+ r_A^- \tag{4}$$

Given the atomic charge operator, the bond order operator, $\hat{I}_{AB}$, is defined as the covariance of the charge operators for centers A and B,[3b,4bc]

$$\hat{I}_{AB} = \alpha(\hat{q}_A - \langle \hat{q}_A \rangle)(\hat{q}_B - \langle \hat{q}_B \rangle) \tag{5}$$

where $\alpha = -2$. Here α is a multiplicative scale factor for normalizing the units. The bond order, I_{AB}, is obtained as the expectation value of the bond order operator, $\hat{I}_{AB}$,

$$I_{AB} = \langle \hat{I}_{AB} \rangle \tag{6}$$

Letting A = B in eq 5 but using a scale factor of 2 leads to the atomic valence for the atom,[4bc,9a]

$$\hat{V}_A = 2(\hat{q}_A - \langle \hat{q}_A \rangle)(\hat{q}_A - \langle \hat{q}_A \rangle) \tag{7}$$

$$V_A = \langle \hat{V}_A \rangle \tag{8}$$

The bonds correlation operator, $\hat{\gamma}_{AB,CD}$, is defined as the covariance of the bond operators for bonds AB and CD,

$$\hat{\gamma}_{AB,CD} = (\hat{I}_{AB} - \langle \hat{I}_{AB} \rangle)(\hat{I}_{CD} - \langle \hat{I}_{CD} \rangle)/\beta \tag{9}$$

where $\beta = [\text{cov}(\hat{I}_{AB}, \hat{I}_{AB}) \cdot \text{cov}(\hat{I}_{CD}, \hat{I}_{CD})]^{1/2}$. The bonds correlation coefficient, $\gamma_{AB,CD}$, is the expectation value of $\hat{\gamma}_{AB,CD}$,

$$\gamma_{AB,CD} = \langle \hat{\gamma}_{AB,CD} \rangle \tag{10}$$

These coefficients for charge (Q_A), bond order (I_{AB}), valence (V_A), and bonds correlation ($\gamma_{AB,CD}$) lead to a hierarchical description of the electronic structure for atoms, molecules, and reactions.

3. Non-Hermitian Problem with Mulliken Charge Operator

Using the Mulliken type charge operator (eq 2), we found that the bonds correlation coefficient sometimes gives unphysical values resulting from a negative self-covariance, $\text{cov}(\hat{I}_{AB}, \hat{I}_{AB})$ and hence, a $\gamma_{AB,CD}$ exceeding the range of -1 to 1. This presumably results from the non-Hermitian nature in the operator. This problem can be illustrated with the computation of atomic valence, V_A (eq 7 and 8).

$$V_A = 2\langle(\hat{q}_A - \langle \hat{q}_A \rangle)(\hat{q}_A - \langle \hat{q}_A \rangle)\rangle \tag{11}$$

V_A is expected to be positive for Hermitian $\hat{q}_A$. However, the Mulliken type atomic charge operator (eq 2) sometimes leads to negative V_A.

For instance, we present results in Table 1 for two H^- anions interacting at very close distances. The first column shows that V_A values computed using the Mulliken $\hat{q}_A$ are negative. We consider that this problem stems from the very definition of $\hat{q}_A$, which is not Hermitian,[12]

$$\hat{q}_A{}^\dagger = \sum_a^A (a^+\bar{a}^-)^\dagger = \sum_a^A \bar{a}^+ a^- \neq \sum_a^A a^+\bar{a}^- = \hat{q}_A \tag{12}$$

We note, however, that the expectation values are the same for $\hat{q}_A$ and $\hat{q}_A{}^\dagger$

$$\langle \hat{q}_A \rangle = \langle \hat{q}_A{}^\dagger \rangle = P_A \tag{13}$$

where

$$P_A = \sum_i^{\text{occ}} n_i C_i^a C_{i,a} \tag{14}$$

In eq 14, $C_{i,a}$ and C_i^a denote covariant and contravariant coefficients for ith molecular orbital, respectively, and n_i is its occupation number.

To understand the non-Hermitian origin problem, we consider the total charge operator, which is Hermitian,

$$\hat{q}_N = \sum_a^N a^+ \bar{a}^- \tag{15}$$

Here N denotes the sum over the entire atomic orbital space (all atoms in the molecule). Equation 15 will be converted to the adjoint representation as follows:

$$\begin{aligned} \hat{q}_N &= \sum_a^N a^+ \bar{a}^- \\ &= \sum_a^N \Big(\sum_{a_1}^N \bar{a}_1^+ S_{a_1 a}\Big)\Big(\sum_{a_2}^N S^{a a_2} a_2^-\Big) \\ &= \sum_a^N \sum_{a_1}^N \sum_{a_2}^N \bar{a}_1^+ a_2^- S_{a_1 a} S^{a a_2} \\ &= \sum_{a_1}^N \sum_{a_2}^N \bar{a}_1^+ a_2^- \Big(\sum_a^N S_{a_1 a} S^{a a_2}\Big) \\ &= \sum_{a_1}^N \sum_{a_2}^N \bar{a}_1^+ a_2^- S_{a_1}^{a_2} \\ &= \sum_{a_1}^N \sum_{a_2}^N \bar{a}_1^+ a_2^- \delta_{a_1 a_2} \\ &= \sum_a^N \bar{a}^+ a^- \\ &= \hat{q}_N{}^\dagger \end{aligned} \tag{16}$$

TABLE 1: Valency, V_A, of H^- in (H^-) Dimer Obtained with Different Definitions of the Charge Operator (R = bond distance)

	charge operator		
R (Å)	Mulliken $\hat{q}_A$	symmetrized Mulliken $\hat{\theta}_A$	NAO $\hat{l}_A$
0.8	−0.218	3.093	0.341
1.0	−0.211	2.440	0.150
1.2	−0.168	2.246	0.067
1.4	−0.122	2.159	0.033
1.6	−0.083	2.107	0.018
1.8	−0.054	2.072	0.010
2.0	−0.032	2.047	0.005

Here S_{ab}, S^{ab}, and S_a^b denote components of overlap matrix in covariant (**S**), contravariant ($\mathbf{S}^{-1}$), and mixed representations, respectively. In eq 16, the summation on a, i.e. $\sum_a^N$, must be complete so that $\sum_a^N S_{a_1 a} S^{a a_2}$ gives $\delta_{a_1 a_2}$. In the atomic charge operator the summation on a, i.e. $\sum_a^A$, is not complete and thus $\hat{q}_A$ is not Hermitian.

We can avoid the negative covariance problem by using a symmetrized atomic charge operator, θ_A,

$$\hat{\theta}_A = \frac{1}{2}\sum_a^A (a^+ \bar{a}^- + \bar{a}^+ a^-) \tag{17}$$

leading to the form

$$V_A = \langle \hat{\theta}_A \hat{\theta}_A \rangle - \langle \hat{\theta}_A \rangle^2 = \frac{1}{4}\sum_a^A (2P_a^a + P_{aa}S^{aa} + P^{aa}S_{aa}) - \frac{1}{2}\sum_{a_1 a_2}^{A,A} (P_{a_1}^{a_2} P_{a_2}^{a_1} + P_{a_1 a_2} P^{a_2 a_1}) \tag{18}$$

The V_A value using eq 18 is presented in the $\hat{\theta}_A$ column of Table 1, where we note that it is always positive. However, the form of the θ_A operator need not define a valence that corresponds to our intuition. Thus, the computed V_A values deviate in this case significantly from rational values.

The non-Hermitian problem could be avoided by using orthogonal atomic orbitals since $\hat{q}_A$ becomes symmetric by definition. Our choice is to use the NAO developed by Weinhold et al.[5]

$$\hat{l}_A = \sum_i^A i^+ \bar{i}^- \quad |i\rangle = |\bar{i}\rangle \tag{19}$$

The results of using NAOs are presented in the third column of Table 1. In this case, the V_A values are all positive and approach zero as the distance between two H^- ions increases. Thus, for CACB calculations, the use of the NAO charge operator is more rigorous than the use of the Mulliken charge operator. Another example showing the problem with non-Hermitian operators is given next.

4. CACB along the Reaction Path

In this section, we study the change in bond orders and bonds correlation coefficients along the reaction path for various systems, with the results in Figures 1−7. We employed the HF wave function and carried out CACB along the intrinsic reaction coordinates (IRC).[13] In the following, the CACB properties have been computed using the NAO charge operator unless otherwise stated. Ab initio calculations were carried out at the HF/6-31G** level of theory using the *Gaussian 94* program.[14]

a. $H + D_2 \rightarrow HD + D$. The hydrogen exchange reaction in Figure 1 is the prototypical bond exchange process,[15] where D is used to help discriminate the hydrogens. Figure 1a shows the energy and bond order profiles along the IRC, and Figure 1b shows the corresponding changes in the bonds correlation coefficients. The bond order changes in Figure 1a illustrate that the forming bond and the breaking bond exchange almost synchronously in the course of the reaction, with $I_{AB}(1) = I_{AB}(2) \approx 0.5$ at the transition state (TS). The bonds correlation between these bonds becomes most negative ($\gamma = -0.173$) also at the TS. The corresponding energy barrier is computed to be 17.9 kcal/mol at the UHF/6-31G** level.

For this reaction, the two end hydrogens have partial bonding interactions [$I_{AB}(3) = 0.051$ at the TS]. This bond is involved in the coupling of the interchanging bonds (1 and 2) and contributes to maintain the total bond order. The figure shows that the total bond order is *conserved* throughout the reaction, slightly exceeding the value of one at the TS ($\Sigma I_{AB} = 1.124$). Since the reaction is covalent by nature, the nonnegligible activation barrier (17.9 kcal/mol) must be explained by certain loss of the total bond order due to the antibonding effect. Thus the increase of the bond order at TS reflects the tendency of the Mayer bond index[3,4] (based on the NAO) to slightly overestimate the bond orders for hypervalent situations such as TS, without including the antibonding effects. Even so, we find that this bond operator leads to useful quantitative characterizations of covalent bond exchange processes.

Figure 2 presents the result for the same reaction with the Mulliken charge operator. Figure 2a shows that the Mulliken charge operator gives bond orders slightly smaller than the NAO charge operator. Consequently, the total bond order decreases slightly below one at the TS, giving an intuitively better picture than NAO. However, the Mulliken charge operator leads to a significant dependence of calculated CACB properties on the basis set being used.[1,16]

Figure 2b shows another problem with the Mulliken charge operator. The correlation coefficients show unphysical behavior, exceeding 1.0 for interactions $\gamma(1,3)$ and $\gamma(2,3)$ at $|R| \cong 1$. This results from the non-Hermitian form of the bond order operator which arises in turn from the non-Hermitian atomic charge operator.

Figure 3 shows the same reaction profile using the Löwdin orthogonalized AO charge operator. Here we see that the unphysical behavior in the Mulliken operator is corrected by this symmetrization of the charge operator.

Generally NAO has the advantage over the Löwdin AOs by preserving locality in atomic orbitals and giving consistent results for extended basis sets.[1,6,16] Thus, we choose to use the NAO charge operator in the CACB formalism.

b. $H_2 + D_2 \rightarrow 2HD$. The $H_2 + D_2$ reaction in Figure 4 describes the symmetry-forbidden 2s+2s reaction where two bonds break and two other bonds form in one step.[17,18] We optimized the D_{4h} TS structure at the HF level using the 6-31G** basis. The singlet RHF wave function has an energy higher than the triplet in the vicinity of the TS. Thus, we used a spin polarized UHF wave function for geometry optimization and for the CACB analysis. Although the UHF wave function has triplet contamination at the TS ($\langle S^2 \rangle = 1.144$), it gives a proper description of bond orders and bonds correlations, leading to continuous behavior along the reaction path.

Figure 4a clearly illustrates that there is only one bonding interaction at the TS. Thus, the total bond order is not conserved, decreasing from 2.000 (initial) to 1.053 (TS), and the corresponding energy barrier is 136.3 kcal/mol (UHF/6-31G**).

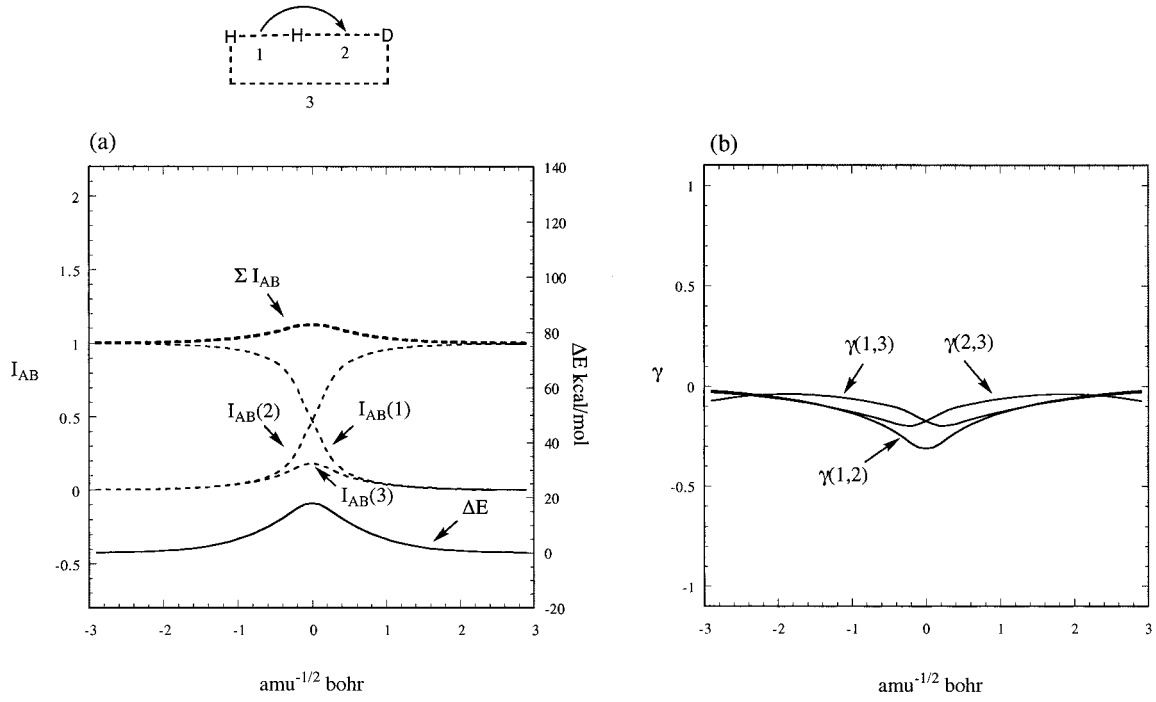

Figure 1. The CACB profile using the NAO charge operator along the reaction coordinate of $H_2 + D \rightarrow HD + H$. (a) Bond orders and HF energy. (b) Bonds correlation coefficients.

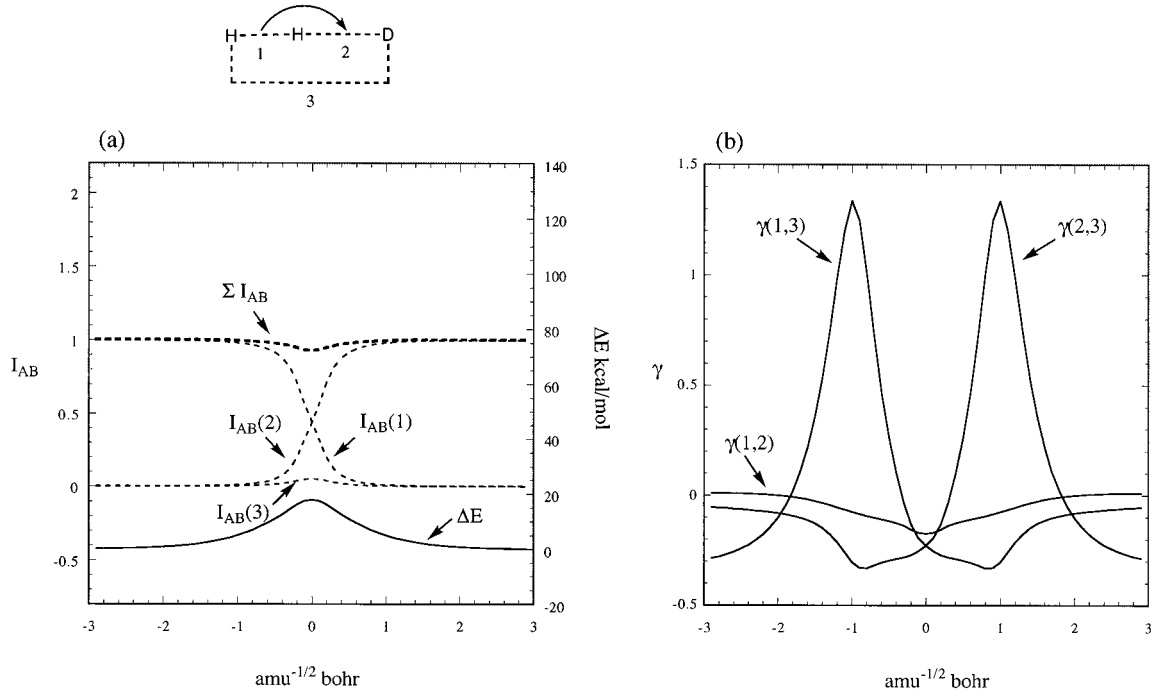

Figure 2. The CACB profile using the Mulliken charge operator along the reaction coordinate of $H_2 + D \rightarrow HD + H$. (a) Bond orders and HF energy. (b) Bonds correlation coefficients.

Consequently, the reaction is forbidden. The loss of virtually one bond order comes from the Pauli principle which does not allow four 1s electrons occupying two mutually orthogonal bonding states at a four-membered TS. In the bond picture, the forming bonds (3 and 4) cannot develop until the breaking bonds (1 and 2) have effectively broken. This leads to a significant increase in the total energy as the two closed-shell electrons come close to each other. Such an antibonding effect is important for proper understanding of the energetics,[19] but the current bond operator only includes covalent bonding effect. (The bond order approaches to zero for both nonbonding and antibonding.) In this picture, the asynchronous bond exchange can be characterized by the intersecting two curves at the TS with much less than half of the original bond order.

The corresponding plot for bonds correlation coefficients in Figure 4b shows that bond exchange coefficients change quite suddenly in the vicinity of the TS as the triplet state mixes to the singlet state. The important bond−bond interactions are between the forming and breaking bonds [$\gamma(1,3)$, $\gamma(1,4)$, $\gamma(2,3)$, and $\gamma(2,4)$], leading to negative correlation at the vicinity of the TS (minimum at TS is −0.296). These coefficients remain zero until very close to the TS, indicating no bond-interchange is allowed for these bonds. The magnitude of the negative coupling is larger in this case than in allowed reaction case (H_2

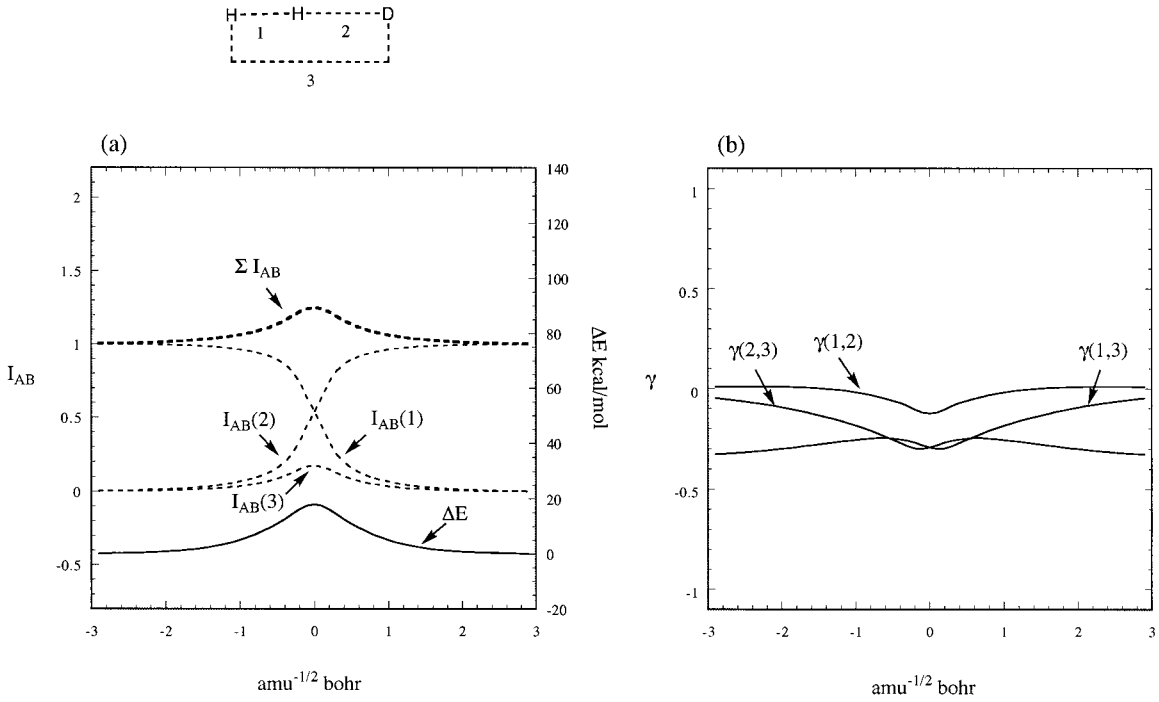

Figure 3. The CACB profile using the Löwdin orthogonal AO charge operator along the reaction coordinate of $H_2 + D \rightarrow HD + H$. (a) Bond orders and HF energy. (b) Bonds correlation coefficients.

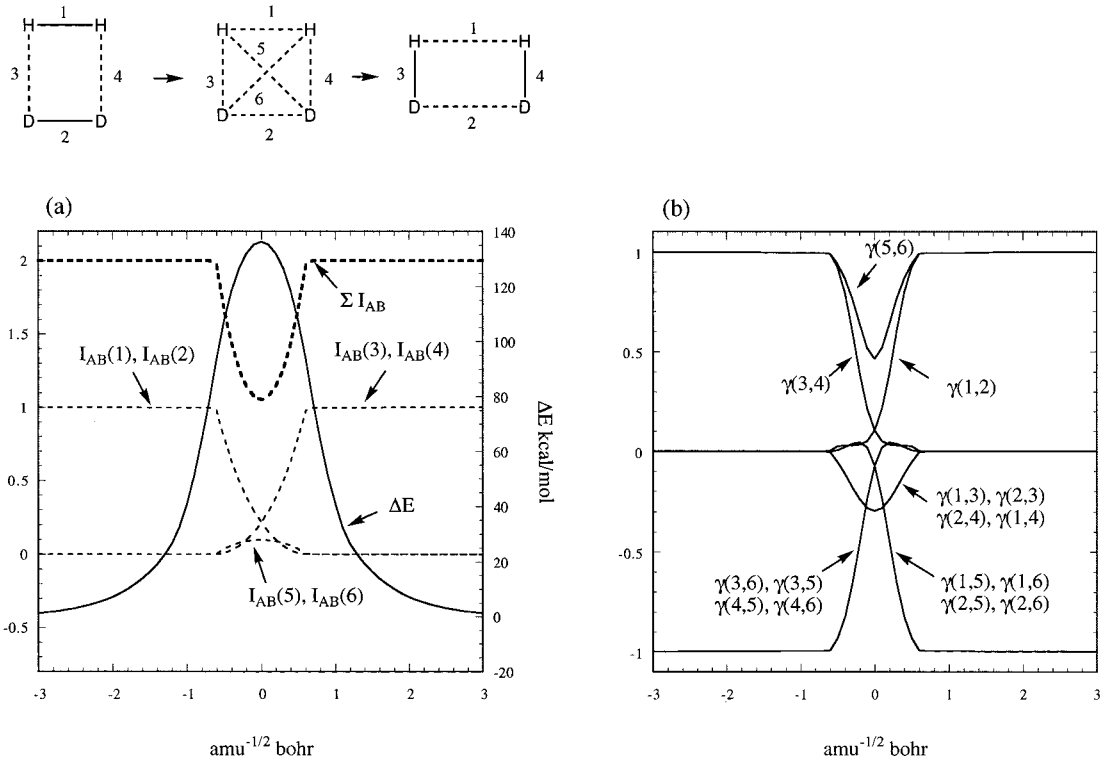

Figure 4. The CACB profile using the NAO charge operator along the reaction coordinate of $H_2 + D_2 \rightarrow HD + HD$. (a) Bond orders and HF energy. (b) Bonds correlation coefficients.

+ D). The bond−bond interaction between parallel bonds [γ(1,2) and γ(3,4)] shows a positive correlation, but only when the corresponding bonds are not developed at all and the value (0.106) is smaller at the TS than the bond exchange coefficients [γ(1,3), γ(1,4), γ(2,3), and γ(2,4)]. These observations are expected to be characteristic of forbidden bond exchange processes.

c. $TiCl_2H^+ + D_2 \rightarrow TiCl_2D^+ + HD$. Figure 5 shows the case of an allowed two-bond exchange process.[20] The bond order and energy profiles in Figure 5 are very different from that in Figure 4. In this case, we have four interchanging bonds (1 to 4) and a weak spectator bond (5). Figure 5 shows that the bond exchange process is perfectly synchronous without any loss of total bond order, ΣI_{AB}. Important bond−bond interactions in this case include adjacent 3-centered correlation, γ(1,4), γ(2,3), γ(1,3), γ(2,4), and parallel correlation γ(1,2), γ(3,4). The bonds correlation between interchanging bonds [γ(1,4), γ(2,3), γ(1,3), γ(2,4)] takes mostly constant value from the beginning to the

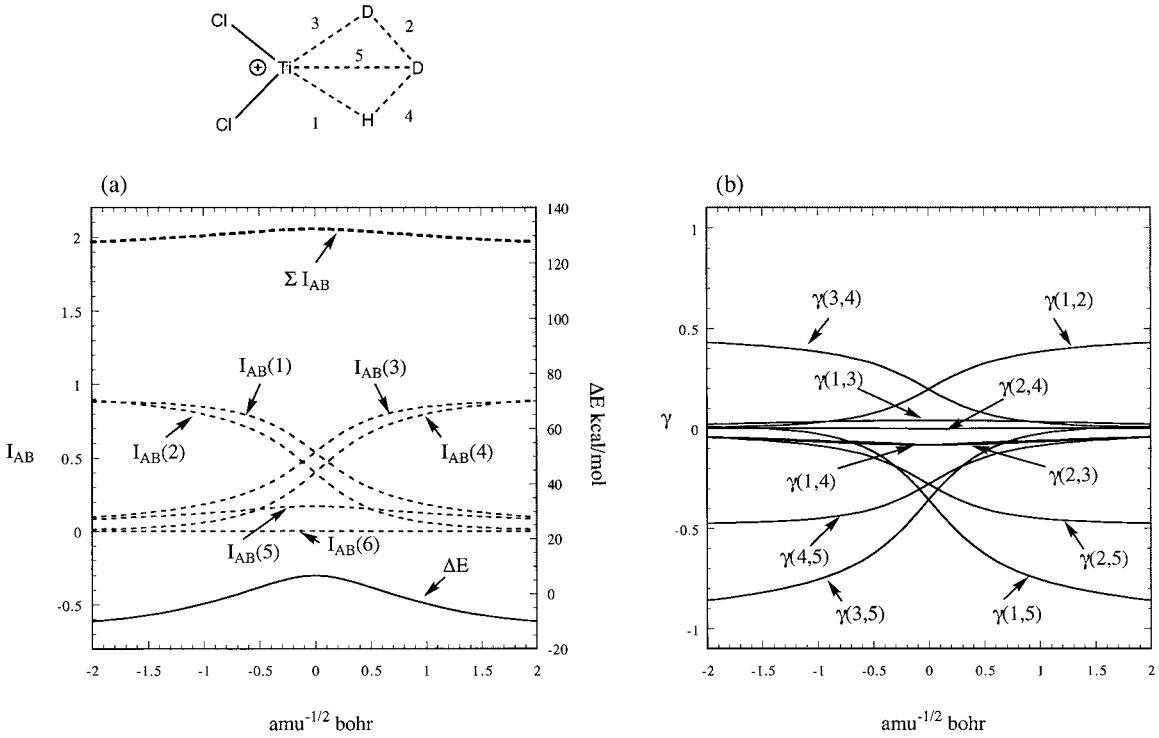

Figure 5. The CACB profile using the NAO charge operator along the reaction coordinate of $TiCl_2H^+ + D_2 \rightarrow TiCl_2D^+ + HD$. (a) Selected bond orders and HF energy. (b) Selected bonds correlation coefficients.

end. These coefficients are $\gamma(1,4)$, $\gamma(2,3) = -0.082$; $\gamma(1,3) = 0.039$; and $\gamma(2,4) = 0.002$ at TS. These small values suggest that the major bond exchanges, (1,4), (2,3), (1,3), and (2,4), take place quite independently. Interpretating the sign of γ(I,J) literally, we may write the real bond exchange only between the Ti−hydrogen and hydrogen−hydrogen bonds. Reflecting

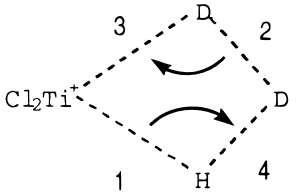

such bond-bond coupling effects, the bond order profile in Figure 5a shows that the bond exchange between 1 and 3 is ahead synchronous (intersects above half of original bond order).

Bonds correlation effects having significant negative value are those with bond 5. The positive couplings between the forming bonds $\gamma(3,4)$ and $\gamma(1,2)$ near the TS work effectively to maintain the total bond order.

Comparing the snapshots of the bond exchange coefficients for H_4 and $TiCl_2H_3^+$ at the TS, the most characteristic difference is in the exchange coefficients for the adjacent bonds. Those coefficients are negative for H_4 (coupled) and rather neutral for $TiCl_2H_3^+$ (independent). In the forbidden case, the coefficients remain near zero until the vicinity of the TS, and then change suddenly to substantial negative values. In the allowed reaction case, the coefficients change gradually and remain near zero through the course of the reaction. The independent simultaneous bond exchange is facilitated by the availability of empty orthogonal atomic orbitals (s^2d^2) at the Ti center.

d. $H_2O + D_2O \rightarrow 2HDO$. In Figure 6 we examine the hydrogen exchange reaction between two water molecules. The reaction is again of 2s+2s type, but the bonds involved here are polar O−H bonds. The reaction might be looked as a proton exchange process.

We optimized the C_{2h} TS structure and confirmed that the structure is a saddle point. The energy profile and the total bond order change in Figure 6 demonstrate that the process is of partially forbidden nature. The activation energy is 58.2 kcal/mol measured from the two isolated water molecules and 62.6 kcal/mol from the dimer complex. Unlike the $H_2 + D_2$ case in section 4.b, the RHF wave function at the TS is stable with respect to the UHF wave function.

As is manifest from the bond order profile, the reaction is not a simple proton exchange process but rather an exchange of two covalent bonds. The bond profile is more similar to the $H_2 + D$ and $TiCl_2H^+ + D_2$ cases than to the $H_2 + D_2$ case. In this case, the bond orders of two breaking bonds, 1 and 2, are 0.73 at the beginning ($R = -4$) and gradually decrease to approximately half of the original value (0.31) at TS ($R = 0$). At the TS, there is an extra oxygen−oxygen interaction, bond 5 ($I_{AB} = 0.09$), which contributes slightly to maintain the total bond order. On the other hand, the hydrogen−hydrogen interaction, bond 6, is negligible.

The bonds correlation profile in Figure 6 shares common features to the $H_2 + D_2$ and $TiCl_2H^+ + D_2$ cases but more resemble the latter. For the H_2O exchange reaction, the important bond−bond interactions are 3-center bond exchange, $\gamma(1,3)$, $\gamma(2,4)$, $\gamma(1,4)$, $\gamma(2,3)$, and parallel bond formation, $\gamma(3,4)$, $\gamma(1,2)$. Note that the 3-center bond exchange coefficients are different between γ_{HOD} and γ_{OHO} (γ_{ODO}), even though the bonds involved are equivalent. These values are rather neutral even at the TS, with a slightly positive γ_{HOD} coefficient (0.06) and a slightly negative γ_{OHO} coefficient (−0.10). This suggests that we consider the bond exchange to take place at the hydrogen center.

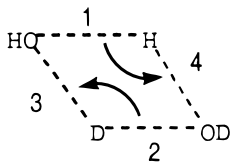

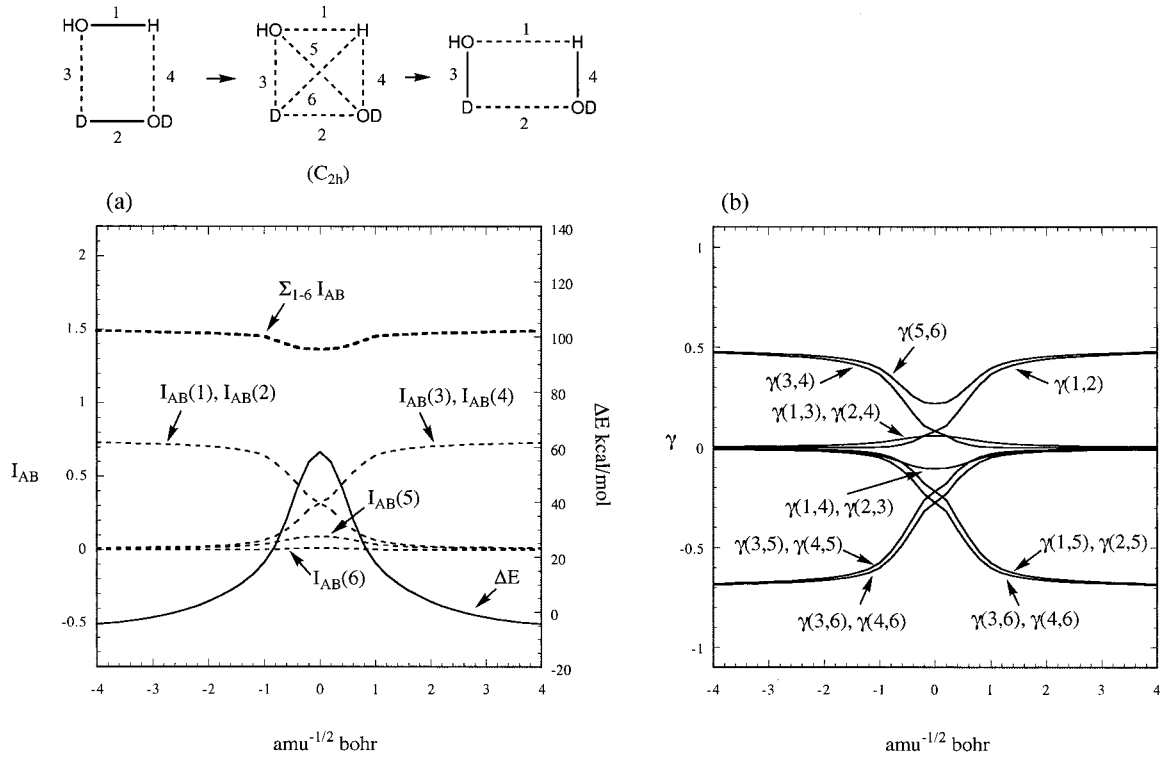

Figure 6. The CACB using the NAO charge operator along the reaction coordinate of $H_2O + D_2O \rightarrow HDO + HDO$. (a) Selected bond orders and HF energy. The total bond order is computed for bonds 1 to 6. (b) Selected bonds correlation coefficients.

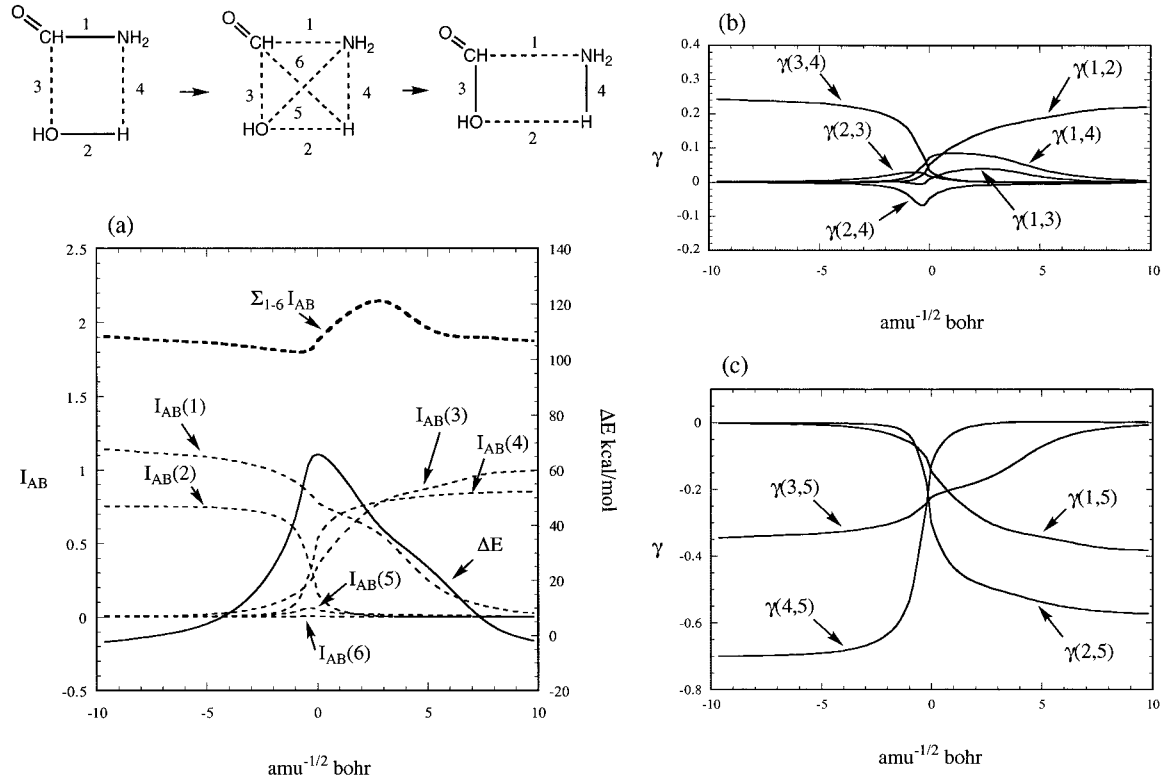

Figure 7. The CACB using the NAO charge operator along the reaction coordinate of $NH_2CHO + H_2O \rightarrow HOCHO + NH_3$. (a) Selected bond orders and HF energy. The total bond order is computed for bonds 1 to 6. (b), (c) Selected bonds correlation coefficients.

Two OH bonds sharing an O center do not possess bond interchanging nature. This independent bond exchange behavior is similar to the $TiCl_2H^+ + D_2$ case.

As in the two other examples for the exchange of two bonds, the parallel bond formations [$\gamma(3,4)$ and $\gamma(1,2)$] accelerate each other. The effect starts only at the nascent phase of forming a bond and nearly vanishes at the TS.

e. $NH_2CHO + H_2O \rightarrow HOCHO + NH_3$. Finally, we consider the hydrolysis of formamide in Figure 7 as another example of a multibond exchange process. The reaction was considered as a prototype for the hydrolysis of a peptide bond, with an activation free energy of 55 kcal/mol estimated by ab initio calculations.[21] Recently, a more plausible base-catalyzed mechanism was studied by high-level ab initio calculations.[22]

Here we reexamine the former process with the CACB formalism.

We optimized the TS structure at the RHF/6-31G** level. The structure is essentially the same as previously reported by Gordon and co-workers.[21] We also confirmed the stability of the singlet RHF wave function at TS.

Figure 7 shows the energy and bond exchange profiles along the IRC. The profile looks like the one for concerted and asynchronous bond exchange processes.[23] Here concerted means that the reactant and the product are connected by a single TS. A stepwise mechanism should include two or more TSs. In this mechanism we have two breaking bonds, C−N (1) and O−H (2), and two newly forming bonds, C−O (3) and N−H (4). The profile suggests that three of these bonds (2, 3, and 4) interchange at the first phase of the reaction. The C−N bond (1) has partial double bond nature as manifest from the bond order exceeding one for a polar bond ($I_{AB} = 1.14$ at $R = -10$) and dissociates rather gradually all the way to the product. After passing the TS the total bond order increases as a new C−O bond (3) gradually develops. Thus, the breaking of C−N bond is rather independent from the formation of other new bonds (vide infra). This is characteristic of reactions in which donor/acceptor type bonds are involved.

The bonds correlation analysis in Figure 7b and 7c confirms the above bond exchange picture, providing additional insight into the interchanging process. Figure 7b shows the adjacent (3-centered) bond exchange [$\gamma(1,3)$, $\gamma(1,4)$, $\gamma(2,3)$, $\gamma(2,4)$] and parallel (4-centered) bond exchange [$\gamma(3,4)$, $\gamma(1,2)$]. In this example, 3-centered bond exchanges are rather independent as was observed for the water dimer case in Figure 6. The only negative coupling is observed for $\gamma(2,4)$. Thus, the bond exchange is effectively H-centered (γ_{OHN}) with two bonds intersecting just before the TS [$\gamma(2,4) = -0.07$ at $R = -0.5$]. The coefficients, $\gamma(2,3)$, $\gamma(1,4)$, and $\gamma(1,3)$ take values of neutral to slightly positive, suggesting that the formation of C−O bond and breaking of the C−N bond are rather independent process to other bonds. Thus, we may write the snapshot at TS as

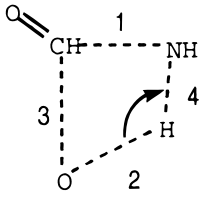

As discussed above such a bond exchange scheme is preferred for a DA bond (in this case the lone pair of the oxygen with the carbonyl carbon, which can accept an extra bond without losing much bonding in other pairs).

The parallel bond−bond acceleration observed here is similar to that found for the water dimer case. The magnitude is smaller than in any other examples, reflecting the independence of bonds in this process.

Figure 7c shows the bonds correlation between the O−N cross bond (5) with other substantial bonds (the bond exchange coefficients are enlarged to more clearly show these effects). The behavior of each bond−bond interaction is similar to other cases studied above. The coefficients $\gamma(3,5)$ and $\gamma(1,5)$ are smaller than $\gamma(4,5)$ and $\gamma(2,5)$, again demonstrating the irrelevance of the bonds 1 and 3 in the exchange.

5. Conclusion

We have demonstrated that the use of a Hermitian charge operator, such as the NAO charge operator, is crucial to obtain physically meaningful values for the CACB properties. The Mulliken type charge operator results in non-Hermitian CACB operators that can give negative atomic valences or correlation coefficients out of boundary (−1 to 1).

The use of the CACB formalism allows new insights into bond exchange processes in chemical reactions. Interchanging bonds have negative coupling in the bonds correlation, reflecting that the one bond is newly forming while the other is breaking. Bond−bond correlation coefficients of this kind have been computed for several prototype reactions, giving neutral to slightly negative values. Such opposite coupling in bond exchange is not significant for allowed reactions of covalent and polar covalent bonds. Thus, the CACB picture of bond exchange is that interchanging bonds are rather independent of each other. Strong bond−bond interactions are observed only at the nascent phase of bond formation and dissociation, not a particularly important region energetically.

To facilitate the use of the CACB analyses for studies by the chemical community, we have made the CACB program available on the Internet.[24] We ask only that users to provide feedback (successes and failures) to improve the program.

Acknowledgment. The MSC thanks Asahi Chemical and NSF (CHE 95-100368) for research funding. The MSC facilities used in this research are supported by grants from NSF-MRI, DOE-ASCI, DOE-MURI, BP Amoco, Chevron Corp., Beckman Institute, Exxon, Seiko-Epson, Owens-Corning, Avery-Dennison, Dow Chemical, and 3M.

References and Notes

(1) Yamasaki, T.; Goddard, W. A., III. *J. Phys. Chem.* **1998**, *102*, 2919.
(2) Wiberg, K. A. *Tetrahedron* **1968**, *24*, 1083.
(3) (a) Giambiagi, M.; de Giambiagi, M. S.; Grempel, D. R.; Heymann, C. D. *J. Chim. Phys.* **1975**, *72*, 15. (b) Giambiagi, M. S.; Giambiagi, M.; Jorge, F. E. *Theor. Chim. Acta* **1985**, *68*, 337. (c) Mundim, K. C.; Giambiagi, M.; de Giambiagi, M. S. *J. Phys. Chem.* **1994**, *98*, 6118.
(4) (a) Mayer, I. *Int. J. Quantum Chem.* **1983**, *23*, 341. (b) Mayer, I. *Chem. Phys. Lett*. **1983**, *97*, 270. (c) Mayer, I. *Int. J. Quantum Chem.* **1986**, *29*, 73. (d) Mayer, I. *Int. J. Quantum Chem*. **1986**, *29*, 477. (e) Mayer, I. *Theor. Chim. Acta* **1985**, *67*, 315. (f) Angyan, J. G.; Michel, L.; Mayer, I. *J. Phys. Chem*. **1994**, *98*, 5244.
(5) Surjan, P. R.; Mayer, I.; Lukovits, I. *Phys. Rev. A* **1985**, *32*, 748.
(6) (a) Reed, A. E.; Weinstock, R. B.; Weinhold, F. *J. Chem. Phys.* **1985**, *83*, 735. (b) Reed, A. E.; Curtiss, L. A.; Weinhold, F. *Chem. Rev.* **1988**, *88*, 899 and references therein.
(7) Bader, R. F. W. *Atoms in Molecules*; Clarendon Press: Oxford, 1994 and references therein.
(8) Baker, J. *Theor. Chim. Acta* **1985**, *68*, 221.
(9) (a) Gopinathan, M. S.; Jug, K. *Theor. Chim. Acta*. **1983**, *63*, 497. (b) Jug, K. *Int. J. Quantum Chem.* **1996**, *60*, 75.
(10) Bachrach, S. M. In *Rev. Comput. Chemistry*; Lipkowitz, K. B., Boyd, D. B., Eds.; VCH: New York, 1993; Vol. 5, p 171 and references therein.
(11) For a general reference to the second quantization and operator algebra, see: (a) Surjan, P. R. *Second Quantized Approach to Quantum Chemistry*; Springer-Verlag: Berlin, Heidelberg, 1989. (b) Jorgensen, P.; Simons, J. *Second Quantization-Based Methods in Quantum Chemistry*; Academic Press: New York, 1981.
(12) Surjan, P. R. *Second Quantized Approach to Quantum Chemistry*; Springer-Verlag: Berlin, Heidelberg, 1989; p 109.
(13) (a) Fukui, K. *Acc. Chem. Res*. **1981**, *14*, 363. (b) Gonzalez, C.; Schlegel, H. B. *J. Chem. Phys*. **1989**, *90*, 2154.
(14) Frisch, M. J.; Trucks, G. W.; Schlegel, H. B.; Gill, P. M. W.; Johnson, B. G.; Robb, M. A.; Cheeseman, J. R.; Keith, T.; Peterson, G. A.; Montgomery, J. A.; Raghavachari, K.; Al-Laham, M. A.; Zakrzewsku, V. G.; Ortiz, J. V.; Foresman, J. B.; Cioslowski, J.; Stefanov, B. B.; Nanayakkara, A.; Challacombe, M.; Peng, C. Y.; Ayala, P. Y.; Chen, W.; Wong, M. W.; Andres, J. L.; Replogle, E. S.; Gomperts, R.; Martin, R. L.; Fox, D. J.; Binkley, J. S.; Defrees, D. J.; Baker, J.; Stewart, J. P.; Head-Gordon, M.; Gonzales, C.; Pople, J. A. *Gaussian 94*, Revision D.1; Gaussian, Inc.: Pittsburgh, PA, 1995.
(15) Goddard, W. A., III; Ladner, R. C. *Int. J. Quantum Chem*. **1969**, *III S*, 63.
(16) Weinhold, F.; Carpenter, J. E. *Theochem*. **1988**, *165*, 189.

(17) Woodward, R. B.; Hoffmann, R. *The Conservation of Orbital Symmetry*; Academic Press: New York, 1970.
(18) (a) Wilson, C. W., Jr.; Goddard, W. A., III. *J. Chem. Phys*. **1969**, *51*, 716. (b) Goddard, W. A., III. *J. Am. Chem. Soc.* **1970**, *92*, 7520. (c) Goddard, W. A., III. *J. Am. Chem. Soc*. **1972**, *94*, 793.
(19) Epiotis, N. D. *Deciphering the Chemical Code: Bonding Across the Periodic Table*, VCH: NewYork, 1996.
(20) Steigerwald, M. L.; Goddard, W. A., III. *J. Am. Chem. Soc.* **1985**, *107*, 5027.
(21) Jensen, J. H.; Baldidge, K. K.; Gordon, M. S. *J. Phys. Chem*. **1992**, *96*, 8340.
(22) Bakowies, D.; Kollman, P. A. *J. Am. Chem. Soc.* **1999**, *121*, 5712.
(23) Dewar, M. J. S. *J. Am. Chem. Soc.* **1984**, *106*, 209.
(24) The URL is http://www.wag.caltech.edu.